

# Evaporation residue cross-sections as a probe for nuclear dissipation in the fission channel of a hot rotating nucleus

Gargi Chaudhuri<sup>a</sup> and Santanu Pal<sup>b</sup>

Variable Energy Cyclotron Centre, 1/AF Bidhan Nagar, Kolkata 700 064, India

Received: 7 March 2003 / Revised version: 30 April 2003 /  
Published online: 30 September 2003 – © Società Italiana di Fisica / Springer-Verlag 2003  
Communicated by W. Henning

**Abstract.** Evaporation residue cross-sections are calculated in a dynamical description of nuclear fission in the framework of the Langevin equation coupled with statistical evaporation of light particles. A theoretical model of one-body nuclear friction which was developed earlier, namely the chaos-weighted wall formula, is used in this calculation for the  $^{224}\text{Th}$  nucleus. The evaporation residue cross-section is found to be very sensitive to the choice of nuclear friction. The present results indicate that the chaotic nature of the single-particle dynamics within the nuclear volume may provide an explanation for the strong shape dependence of nuclear friction which is usually required to fit experimental data.

**PACS.** 05.40.Jc Brownian motion – 24.60.Lz Chaos in nuclear systems – 25.70.Gh Compound nucleus – 25.70.Jj Fusion and fusion-fission reactions

## 1 Introduction

Fission of highly excited compound nuclei produced in heavy-ion-induced fusion reactions has evoked considerable interest in the recent years mainly due to the fact that it cannot be accounted for by the statistical model of Bohr and Wheeler for nuclear fission [1]. In particular, it is now established that the multiplicities of neutrons, light charged particles and photons emitted by a hot compound nucleus are much higher than those predicted by the statistical model [2]. This implies that the fission lifetime is considerably underestimated when using the Bohr-Wheeler description of nuclear fission. Consequently, dissipative dynamical models for fission of excited nuclei were developed following the original work of Kramers who considered fission dynamics to be analogous to that of diffusion of Brownian particles over a barrier [3]. These dynamical models were found to be successful in reproducing a large body of experimentally measured multiplicity data [4, 5].

Dynamical effects are also found essential to calculate the evaporation residue cross-section of highly excited compound nuclei [6]. Specifically, the decay width for an overdamped system was subsequently found to be more appropriate for nuclear fission and this fission width is generally used in the description of the statistical decay

of an excited compound nucleus [7, 8]. It turns out that the evaporation residue cross-section depends strongly on the strength of the nuclear dissipation whenever it is a very small fraction of the total fusion cross-section. In fact, the evaporation residue cross-section in such cases can serve the purpose of a sensitive probe for nuclear dissipation.

The dissipative force in the dynamics of fission arises due to the interaction between the large number of intrinsic nuclear degrees of freedom and the few collective or fission degrees of freedom. The strength of the dissipative force is usually treated as an adjustable parameter in order to fit the experimental data. Fröbrich *et al.* [9] obtained a phenomenological shape-dependent nuclear dissipation which was able to reproduce the fission probability and pre-scission neutron multiplicity excitation functions for a number of compound nuclei. The magnitude of this phenomenological dissipation was found to be very small for compact shapes of the nucleus, but a strong increase in its value was needed for large deformations. In a recent work, Diószegi *et al.* [8] have analyzed the  $\gamma$  as well as neutron multiplicities and evaporation residue cross-section of  $^{224}\text{Th}$  and have concluded that the experimental data can be fitted equally well with either a temperature- or a deformation-dependent nuclear dissipation. Interestingly, the deformation dependence of the above dissipation also corresponds to a lower value of the strength of the dissipation inside the saddle and a higher value outside the saddle, similar to the phenomenological dissipation of ref. [9] mentioned above.

<sup>a</sup> e-mail: [gargi@veccal.ernet.in](mailto:gargi@veccal.ernet.in)

<sup>b</sup> e-mail: [santanu@veccal.ernet.in](mailto:santanu@veccal.ernet.in)

A theoretical model for nuclear dissipation, namely the wall formula, was developed long ago by Blocki *et al.* [10] in a simple classical picture of one-body dissipation. However, the strength of the wall dissipation was found to be considerably higher than that required to fit experimental data. It is only recently that a modification has been incorporated into the wall formula which resulted in a shape-dependent reduction factor in the strength of the friction [11]. The modification essentially arose out of a closer examination of one crucial assumption of the wall formula concerning the randomization of particle motion within the nuclear volume. It was assumed in the original wall formula that the particle motion is fully randomized. This full randomization assumption is relaxed in the modified wall formula in order to make it applicable to systems with partly randomized or chaotic single-particle motion. In what follows, we shall use the term ‘‘chaos-weighted wall formula’’ (CWWF) for this modified dissipation in order to distinguish it from the original wall formula (WF) dissipation. As was shown in ref. [11], the CWWF dissipation coefficient  $\eta_{\text{cwwf}}$  will be given as

$$\eta_{\text{cwwf}} = \mu\eta_{\text{wf}}, \quad (1)$$

where  $\eta_{\text{wf}}$  is the dissipation or friction coefficient as was given by the original wall formula [10] and  $\mu$  is a measure of chaos (chaoticity) in the single-particle motion and depends on the instantaneous shape of the nucleus. The value of chaoticity  $\mu$  changes from 0 to 1 as the nucleus evolves from a spherical shape to a highly deformed one. The CWWF dissipation is thus much smaller than the WF dissipation for compact nuclear shapes while they become closer at large deformations. It is worthwhile noting here that the above shape-dependent CWWF has features similar to the empirical dissipations discussed in the last paragraph. In a recent work, we have shown that the precission neutron multiplicity and fission probability calculated from Langevin dynamics using the chaos-weighted wall dissipation agree fairly well with the experimental data for a number of heavy compound nuclei ( $A \sim 200$ ) over a wide range of excitation energies [12]. This strongly suggests that the shape-dependent CWWF can be considered as a suitable theoretical model for one-body dissipation in nuclear fission. Further, a lack of full randomization or chaos in the single-particle motion can provide a physical explanation for the empirical requirement for reduction in strength of friction for compact nuclear shapes in order to fit experimental data.

In the present work, we shall employ the chaos-weighted wall formula dissipation to calculate the evaporation residue excitation function for the  $^{224}\text{Th}$  nucleus. Our main motivation here will be to put the chaos-weighted wall formula to a further test and verify to what extent it can account for the experimental evaporation residue data which is a very sensitive probe for nuclear dissipation. In our calculation, we shall first assume that a compound nucleus is formed when a projectile nucleus completely fuses with a target nucleus in a heavy-ion collision. Processes such as fast fission or quasifission thus cannot be described in the model considered here. We shall describe the fission

dynamics of the compound nucleus by the Langevin equation while the light particles and photons will undergo statistical emission. The Langevin equation will be solved by coupling it with particle and  $\gamma$  evaporation at each step of its time evolution. The precission particle multiplicity and fission probability will be obtained by sampling over a large number of Langevin trajectories. The chaos-weighted wall friction coefficient is obtained following a specific procedure [14] which explicitly considers particle dynamics in phase space in order to calculate the chaoticity factor  $\mu$  of eq. (1). There is no free parameter in this calculation of friction. The other input parameters for the dynamical calculation are obtained from standard nuclear models. Calculation will be performed at a number of excitation energies for  $^{224}\text{Th}$  formed in the  $^{16}\text{O} + ^{208}\text{Pb}$  system. We have chosen this system essentially because of the availability of experimental data on both evaporation residue and precission neutron multiplicity covering the same range of excitation energies and the fact that earlier analyses of the evaporation residue excitation function have already indicated the need for a dynamical model for fission of this nucleus [15–17].

In the following section, we shall briefly describe the dynamical model along with the necessary input as used in the present work. The details of the calculation will also be given here. The calculated evaporation residue excitation function and precission neutron multiplicities will be compared with the experimental values in sect. 3. A summary of the results along with the conclusions can be found in the last section.

## 2 Langevin description of fission

An appropriate set of collective coordinates to describe the fission degree of freedom consists of the shape parameters  $c$ ,  $h$  and  $\alpha$  as was suggested by Brack *et al.* [18] and we shall employ them in the present calculation. We further simplify our calculation by considering only symmetric fission ( $\alpha = 0$ ) since the compound nucleus  $^{224}\text{Th}$  is much heavier than the Bussinaro-Gallone transition point. The potential landscape in  $(c, h)$  coordinates is generated from the finite-range liquid-drop model [19] where we calculate the generalized nuclear energy by double-folding the uniform density with a Yukawa-plus-exponential potential. The Coulomb energy is obtained by double-folding another Yukawa function with the density distribution. We shall further assume in the present work that fission would proceed along the valley of the potential energy landscape. Consequently, we shall use an effective one-dimensional potential in the Langevin equation which will be defined as  $V(c) = V(c, h)$  *at valley*. This will reduce the problem to one dimension in order to simplify the computation. The Langevin equations in one dimension will thus be given [20] as

$$\begin{aligned} \frac{dp}{dt} &= -\frac{p^2}{2} \frac{\partial}{\partial c} \left( \frac{1}{m} \right) - \frac{\partial F}{\partial c} - \eta\dot{c} + R(t), \\ \frac{dc}{dt} &= \frac{p}{m}. \end{aligned} \quad (2)$$

The shape-dependent collective inertia and the dissipation coefficients in the above equations are denoted by  $m$  and  $\eta$ , respectively.  $F$  is the free energy of the system while  $R(t)$  represents the random part of the interaction between the fission degree of freedom and the rest of the nuclear degrees of freedom considered collectively as a thermal bath in the present picture. The collective inertia,  $m$ , will be obtained by making the Werner-Wheeler approximation [21] assuming an incompressible irrotational flow. The driving force in a thermodynamic system should be derived from its free energy which we will calculate considering the nucleus as a noninteracting Fermi gas [9]. The instantaneous random force  $R(t)$  is assumed to have a stochastic nature with a Gaussian distribution whose average is zero [4]. The strength of the random force will be determined by the dissipation coefficient through the fluctuation-dissipation theorem. The various input quantities are described in some detail in a recent publication [12].

## 2.1 Nuclear dissipation

We shall use the chaos-weighted one-body wall-and-window dissipation in the present calculation. We shall briefly describe here the essential features of this dissipation, the details of which may be found elsewhere [12]. In the wall-and-window model of one-body dissipation, the window friction is expected to be effective after a neck is formed in the nuclear system [22]. Further, the radius of the neck connecting the two future fragments should be sufficiently narrow in order to make the energy transfer irreversible. It therefore appears that the window friction should be very nominal when neck formation just begins. Its strength should increase as the neck becomes narrower reaching its classical value when the neck radius becomes much smaller than the typical radii of the fragments. We shall approximately describe the above scenario by defining a transition point  $c_{\text{win}}$  in the elongation coordinate at which the window friction will be turned on. We shall also assume that the compound nucleus evolves into a binary system beyond  $c_{\text{win}}$  and accordingly correction terms for the motions of the centers of mass of the two halves will be applied to the wall formula for  $c > c_{\text{win}}$  [22]. However, it may be noted that the window dissipation and the center-of-mass motion correction tend to cancel each other to some extent. Consequently, the resulting wall-and-window friction is not very sensitive to the choice of the transition point. We shall choose a value for  $c_{\text{win}}$  at which the nucleus has a binary shape and the neck radius is half of the radius of either of the would-be fragments.

The wall-and-window dissipation and its chaos-weighted version will thus be given as

$$\eta_{\text{wf}}(c < c_{\text{win}}) = \eta_{\text{wall}}(c < c_{\text{win}}), \quad (3)$$

and

$$\eta_{\text{wf}}(c \geq c_{\text{win}}) = \eta_{\text{wall}}(c \geq c_{\text{win}}) + \eta_{\text{win}}(c \geq c_{\text{win}}), \quad (4)$$

while

$$\eta_{\text{cwwf}}(c < c_{\text{win}}) = \mu(c)\eta_{\text{wall}}(c < c_{\text{win}}), \quad (5)$$

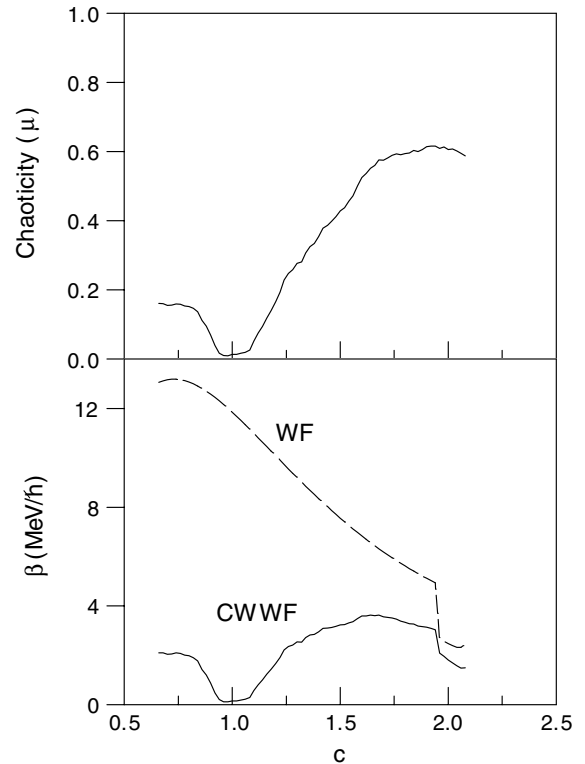


**Fig. 1.** Shape dependence of chaoticity  $\mu$ , the reduction factor in chaos-weighted wall friction (upper panel), and the reduced friction  $\beta$  (lower panel) for  $^{224}\text{Th}$ .

and

$$\eta_{\text{cwwf}}(c \geq c_{\text{win}}) = \mu(c)\eta_{\text{wall}}(c \geq c_{\text{win}}) + \eta_{\text{win}}(c \geq c_{\text{win}}). \quad (6)$$

The detailed expressions for the wall-and-window frictions can be found in ref. [22].

The chaoticity  $\mu(c)$ , introduced in the previous section, depends on the instantaneous shape of the nucleus [11]. In a classical picture, this will be given as the average fraction of the nucleon trajectories within the nucleus which are chaotic when the sampling is done uniformly over the nuclear surface. The value of the chaoticity for a given nuclear shape is evaluated by sampling over a large number of classical nucleon trajectories while each trajectory is identified either as a regular or as a chaotic one by considering the magnitude of its Lyapunov exponent and the nature of its variation with time [14]. The shape dependence of the chaoticity, thus obtained, is shown in fig. 1. Further, defining the quantity  $\beta(c) = \eta(c)/m(c)$  as the reduced dissipation coefficient, its dependence on the elongation coordinate is also shown in fig. 1 for the  $^{224}\text{Th}$  nucleus. It can be immediately noticed that the CWWF is strongly suppressed compared to the WF dissipation for near-spherical shapes ( $c \sim 1$ ) and this can be qualitatively understood as follows. A particle moving in a spherical mean field represents a typical integrable system and its dynamics is completely regular. When the boundary of the mean field is set into motion (as in fission), the energy gained by the particle at one instant as a result of a collision with the moving boundary is eventually fed back to the

boundary motion in the course of later collisions. An integrable system thus becomes completely nondissipative in this picture resulting in a vanishing dissipation coefficient. It may be noted that the suppression of friction strength in CWWF is qualitatively similar to the shape-dependent frictions found empirically [8,9] to fit experimental data. The considerations of chaos (or rather lack of it) in particle motion can thus provide a physical explanation for the reduction in friction strength required for compact shapes of the compound nucleus.

The strong shape dependence of the CWWF can have some interesting consequences. In a dynamical description of fission, a compound nucleus spends most of its time in undergoing shape oscillations in the vicinity of its ground-state shape before it eventually crosses the saddle and proceeds towards the scission point. Since the spin of a compound nucleus formed at a small excitation is also small, its ground-state shape is nearly spherical and in this region the CWWF friction is also small. Conversely, higher spin values are mostly populated in a highly excited compound nucleus making its ground-state shape highly deformed and thus it experiences a strong CWWF friction. Therefore, if one uses a shape-independent friction in a dynamical model of fission, its strength has to increase with increasing temperature, in order to give an equivalent description to that provided by the temperature-independent but shape-dependent CWWF friction. In fact, it was observed in ref. [8] that a shape-dependent friction fits the experimental data equally well as achieved by a strong temperature-dependent friction. Since there is a physical justification for shape dependence in nuclear friction from chaos considerations, it is quite likely that the above strong temperature dependence, at least a substantial part of it, is of dynamical origin as explained above and thus is an artifact arising out of using a shape-independent friction.

It must be pointed out, however, that one would expect a temperature dependence of nuclear friction from general considerations such as larger phase space becoming accessible for particle-hole excitations at higher temperatures. In a microscopic model of nuclear friction using nuclear response function, Hofmann *et al.* [13] have obtained a nuclear friction which depends upon temperature as  $0.6T^2$  (leading term). This may be compared with the empirical temperature-dependent term of  $3T^2$  which was found in ref. [8]. It therefore appears that only a small fraction of the empirical temperature dependence can be accounted for by the inherent temperature dependence of nuclear friction, while the rest of it has a dynamical origin as we have discussed above.

In the present work, we shall not consider any empirical temperature dependence of the CWWF or WF frictions in order to study solely the effects of shape dependence. In what follows, we shall use both the WF and CWWF dissipations in a dynamical model of fission and shall investigate the effect of the reduction in the CWWF strength on the evaporation residue cross-section.

## 2.2 Dynamical model calculation

In the dynamical model calculation, the initial spin and excitation energy of the compound nucleus is determined from the entrance channel specifications in the following manner. The fusion cross-section of the target and projectile in the entrance channel usually obeys the following spin distribution:

$$\frac{d\sigma(l)}{dl} = \frac{\pi}{k^2} \frac{(2l+1)}{1 + \exp\left(\frac{l-l_c}{\delta l}\right)}, \quad (7)$$

where we shall obtain the parameters  $l_c$  and  $\delta l$  by fitting the experimental fusion cross-sections. The initial spin of the compound nucleus in our calculation will be obtained by sampling the above spin distribution function. The total excitation energy ( $E^*$ ) of the compound nucleus can be obtained from the beam energy of the projectile, and energy conservation in the form

$$E^* = E_{\text{int}} + V(c) + p^2/2m \quad (8)$$

gives the intrinsic excitation energy  $E_{\text{int}}$  and the corresponding nuclear temperature  $T = (E_{\text{int}}/a)^{1/2}$ , where  $a$  is the nuclear level density parameter. The centrifugal potential is included in  $V(c)$  in the above equation.

We shall use the following level density parameter due to Ignatyuk *et al.* [23] which incorporates the nuclear shell structure at low excitation energy and goes smoothly to the liquid-drop behavior at high excitation energy,

$$a(E_{\text{int}}) = \bar{a} \left( 1 + \frac{f(E_{\text{int}})}{E_{\text{int}}} \delta M \right), \quad (9)$$

with

$$f(E_{\text{int}}) = 1 - \exp(-E_{\text{int}}/E_D),$$

where  $\bar{a}$  is the liquid-drop level density parameter,  $E_D$  determines the rate at which the shell effects disappear at high excitations, and  $\delta M$  is the shell correction given by the difference between the experimental and liquid-drop masses, ( $\delta M = M_{\text{exp}} - M_{\text{LDM}}$ ). We shall further use the shape-dependent liquid-drop level density parameter given as [24]

$$\bar{a}(c) = a_v A + a_s A^{2/3} B_s(c), \quad (10)$$

where we choose the values for the parameters  $a_v$ ,  $a_s$  and the dimensionless surface area  $B_s$  following ref. [9].

In order to solve the Langevin equations, the initial values of the coordinates and momenta ( $c, p$ ) of the fission degree of freedom are obtained from sampling random numbers following the Maxwell-Boltzmann distribution. The Langevin equations (eq. (2)) are subsequently numerically integrated following the procedure outlined in ref. [4]. At each time step of integration of the Langevin equations, particle (neutron, proton and alpha) and giant dipole  $\gamma$  evaporation will be considered following a Monte Carlo sampling technique [9]. For this purpose, the particle and  $\gamma$  decay widths are calculated using the inverse cross-section formula as given in ref. [5]. After each particle emission, the potential energy landscape of the parent nucleus is

replaced by that of the daughter nucleus. The intrinsic excitation energy, mass and spin of the compound nucleus are also recalculated after each emission. The spin of the compound nucleus is reduced only in an approximate way by assuming that each neutron, proton or a  $\gamma$  carries away  $1\hbar$  angular momentum, while that carried by an alpha particle is  $2\hbar$ . However, only neutron emission is found to be relevant for the yield of the residue cross-section.

A Langevin trajectory will be considered as having undergone fission if it reaches the scission point ( $c_{sci}$ ) in course of its time evolution. Alternately, it will be counted as an evaporation residue event if the intrinsic excitation energy becomes smaller than either the fission barrier or the binding energy of a particle. The calculation proceeds until the compound nucleus undergoes fission or becomes an evaporation residue. This calculation is repeated for a large number of Langevin trajectories and the evaporation residue formation probability is obtained as the fraction of the trajectories which have ended up as evaporation residues. The evaporation residue cross-section is subsequently obtained by multiplying the experimental value for fusion cross-section in the entrance channel with the above formation probability of the evaporation residue. Similarly, the average number of particles (neutrons, protons or alphas) emitted in the fission events will give the required precession particle multiplicities.

Following the fission dynamics through the Langevin equation during the entire lifetime of a compound nucleus can however take an extremely long computer time. As an alternative procedure, we shall first follow the time evolution of a compound nucleus according to the Langevin equations for a sufficiently long period during which a steady flow across the fission barrier is established. Beyond this period, a statistical model for compound nucleus decay is expected to be equally valid and more economical in terms of computation. We shall therefore switch over to a statistical model description after the fission process reaches the stationary regime. This combined dynamical and statistical model, first proposed by Mavlitov *et al.* [25], however, requires the fission width along with the particle and  $\gamma$  widths in the statistical branch of the calculation. This fission width should be the stationary limit of the fission rate as determined by the Langevin equation. However, it is not possible to obtain this fission rate analytically for the strongly shape-dependent CWWF and WF dissipations. We shall therefore use a suitable parametric form of the numerically obtained stationary fission widths using the CWWF (and also WF) dissipations in order to use them in the statistical branch of our calculation. The details of this procedure are given in ref. [26] which we shall follow to calculate all the required fission widths for the present work.

### 3 Results

We have calculated the precession neutron multiplicity and the evaporation residue (ER) cross-section for the compound nucleus  $^{224}\text{Th}$  when it is formed in the fusion of an incident  $^{16}\text{O}$  nucleus with a  $^{208}\text{Pb}$  target nucleus.

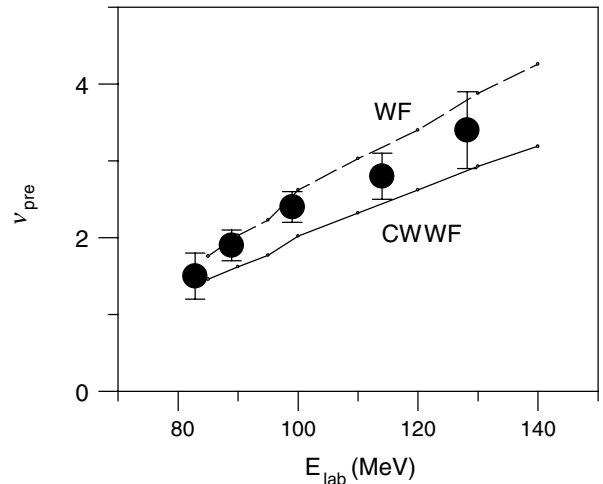


**Fig. 2.** Precession neutron multiplicity ( $\nu_{pre}$ ) excitation function calculated with WF (dashed line) and CWWF (full line) frictions for the reaction  $^{16}\text{O} + ^{208}\text{Pb}$ . The experimental points (dots) are also shown.

The calculation is done at a number of incident energies in the range of 80 MeV to 140 MeV using both the WF and the CWWF dissipations. Figure 2 shows the calculated precession neutron multiplicity along with the experimental data [15]. Both the WF and CWWF predictions for multiplicity are quite close to the experimental values and this shows that neutron multiplicity is not very sensitive to the dissipation in fission in the energy range under consideration. It must be pointed out, however, that the CWWF predictions for neutron multiplicity are closer to experimental data compared to those from WF at much higher excitations of the compound nucleus [12].

It may be mentioned at this point that though we calculate the number of precession protons, alphas and GDR  $\gamma$ 's, we do not compare them with experimental data because these numbers are rather small with large statistical uncertainties in the present work. In order to obtain the energy spectrum of the  $\gamma$  multiplicity with a reasonable statistical accuracy, in particular, it is necessary to perform computation using a much larger ensemble of trajectories than the one (comprising of 20000 trajectories) used here. This puts a severe demand on computer time making such computations impractical at present. However, an alternative approach would be to make use of the time-dependent fission widths in a full statistical model calculation of the compound nucleus decay. This calculation would be much faster than the present Langevin dynamical model calculation though the time-dependent fission widths would be required as input to this statistical model calculation. We plan to perform such calculations in future.

We shall next consider the results of the evaporation residue calculation. Figure 3 shows the evaporation residue excitation functions calculated using both the WF and CWWF dissipations. The experimental values of evaporation residue cross-section are also shown in this figure [17]. We first note that the calculated evaporation

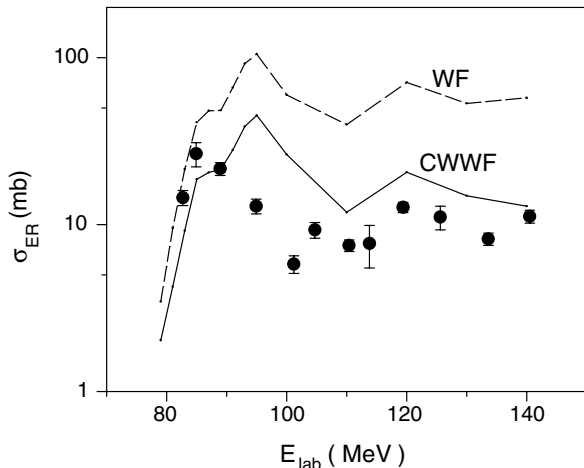


**Fig. 3.** Evaporation residue cross-section excitation function calculated with WF (dashed line) and CWWF (full line) frictions for the reaction as in fig. 2. The experimental points (dots) are also shown.

residue cross-section is very sensitive to the dissipation in the fission degree of freedom. The WF predictions are a few times (typically 2-5) larger than those obtained with the CWWF dissipation. Next, we make the important observation that the CWWF predicted excitation function is much closer to the experimental values than that obtained with the WF dissipation. This observation clearly shows that the chaos-weighted factor in CWWF changes its strength in the right direction. We must take note of the fact, however, that the CWWF still considerably overestimates the ER cross-section. Since the present dynamical calculation considers only one (elongation) fission degree of freedom, it is expected that inclusion of the neck degree of freedom will increase the fission probability [27] further and hence reduce the ER cross-section. We plan to extend our work in this direction in future. We further observe that while a peak appears in the experimental excitation function at about 85 MeV, the same is shifted by 10 MeV in the calculated results. We do not have any explanation for this discrepancy except pointing out that there is no free parameter in our calculation and thus no parameter tuning has been attempted in order to fit experimental data. A similar shift has also been observed in an earlier work [8].

The structure of the evaporation residue excitation function can also reveal certain interesting features. Since the calculated values of the evaporation residue cross-section are obtained as the product of the fusion cross-section and the probability of evaporation residue formation, the initial rise of the ER cross-section with beam energy essentially reflects the steep rise of fusion cross-section in this energy region [16]. At still higher beam energies, the ER cross-section becomes approximately stable which results from a delicate balance between the increasing trend of the fusion cross-section and the decreasing trend of the probability of ER formation. Had the ER formation probability decreased at a rate higher than those obtained in the present calculation, the resulting ER

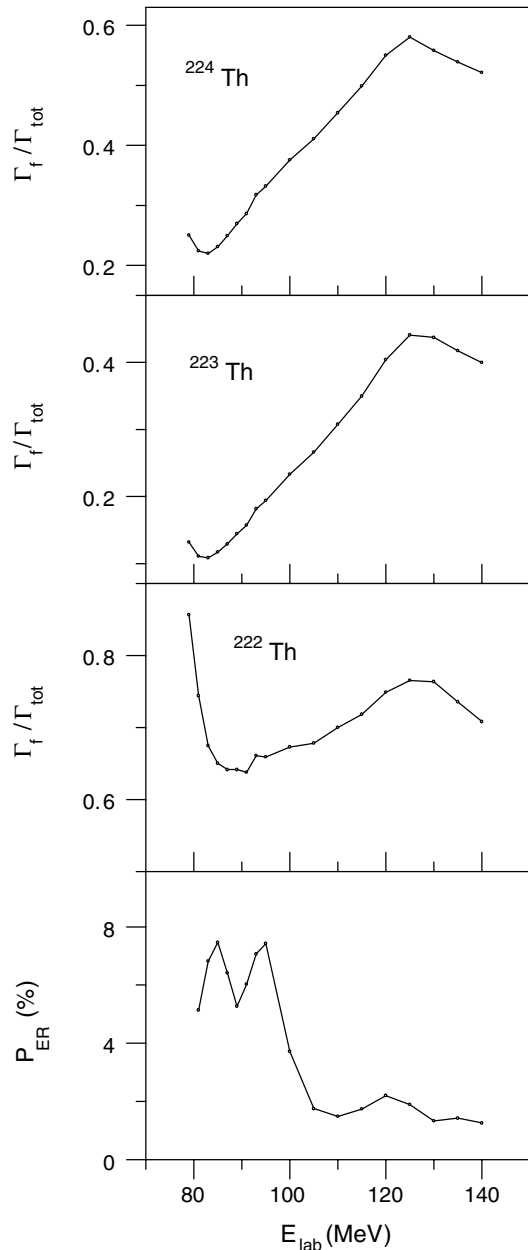


**Fig. 4.** The top three panels show the fission partial widths for  $^{224}\text{Th}$ ,  $^{223}\text{Th}$  and  $^{222}\text{Th}$  (see text). The total width  $\Gamma_{\text{tot}}$  includes the neutron, proton, alpha and  $\gamma$  evaporation widths in addition to the fission width. The bottom panel displays the excitation function of the evaporation residue formation probability for the reaction as in fig. 2.

cross-section would have decreased at higher compound nuclear excitations. In fact, such an observation was made in ref. [17], where the ER cross-section obtained from standard statistical model calculation was found to decrease very steeply beyond 100 MeV of beam energy. In order to explore this point a little further, we have calculated the excitation function of the partial width for fission. Since fission can take place at any stage during neutron (or any other light particle) evaporation, the partial widths are calculated for  $^{222}\text{Th}$  and  $^{223}\text{Th}$  as well at excitation

energies reduced by the neutron separation energy after each neutron emission. The compound nuclear spin was taken as  $l_c$  from eq. (7) while only CWWF dissipation was considered for this calculation.

The calculated excitation functions of the fission partial widths are shown in fig. 4. The calculated values of the ER formation probability ( $P_{ER}$ ) are also displayed in this figure. Each partial width excitation function is found to have a minimum around 90 MeV of beam energy after which it starts increasing till this trend is arrested and reversed at higher excitations. Recalling the fact that the above results on partial widths are only indicative while  $P_{ER}$  is obtained from a full dynamical calculation, it is of interest to note that a bump in the excitation function of  $P_{ER}$  also appears in the above ( $\sim 90$  MeV) energy range. Subsequently, the value of  $P_{ER}$  drops rather sharply before it settles to a steady value at higher excitations. This feature is also complementary to that of the excitation functions of the partial widths of fission. We thus demonstrate in a schematic manner how the structure in the excitation function of the ER cross-section is related to the competition between fission and other decay channels at different stages of fission.

## 4 Summary and conclusions

We have applied a theoretical model of one-body nuclear friction, namely the chaos-weighted wall formula, to a dynamical description of compound nuclear decay where fission is governed by the Langevin equation coupled with the statistical evaporation of light particles. We have used both the standard wall formula and its modified form with the chaos-weighted factor in order to calculate the pre-scission neutron multiplicity and evaporation residue excitation functions for the  $^{224}\text{Th}$  nucleus. Though the number of the pre-scission neutrons calculated with either WF or CWWF friction are found to be very close to each other in the energy range considered, the evaporation residue cross-section is found to depend very strongly on the choice of nuclear friction. The evaporation residue cross-section calculated with the CWWF friction gives a much better agreement with the experimental data compared to the WF predictions. This result demonstrates that the consequences of chaos in particle motion give rise to a strong suppression of the strength of the wall friction for compact shapes of the compound nucleus which, in turn, brings theoretically calculated evaporation residue cross-sections considerably closer to the experimental values. Thus the chaos considerations may provide a plausible explanation for the shape dependence of the strength of nuclear friction which was found [8,9] to be necessary in order to fit experimental data.

## References

1. N. Bohr, J.A. Wheeler, Phys. Rev. **56**, 426 (1939).
2. M. Thoennessen, G.F. Bertsch, Phys. Rev. Lett. **71**, 4303 (1993).
3. H.A. Kramers, Physica (Amsterdam) **4**, 284 (1940).
4. Y. Abe, S. Ayik, P.-G. Reinhard, E. Suraud, Phys. Rep. **275**, 49 (1996).
5. P. Fröbrich, I.I. Gontchar, Phys. Rep. **292**, 131 (1998).
6. D. Fabris, G. Viesti, E. Fioretto, M. Cinausero, N. Gelli, K. Hagel, F. Lucarelli, J.B. Natowitz, G. Nebbia, G. Prete, R. Wada, Phys. Rev. Lett. **73**, 2676 (1994).
7. B.B. Back, D.J. Blumenthal, C.N. Davids, D.J. Henderson, R. Hermann, D.J. Hofman, C.L. Jiang, H.T. Pentilä, A.H. Wuosmaa, Phys. Rev. C **60**, 044602-1 (1999).
8. I. Díószegi, N.P. Shaw, I. Mazumdar, A. Hazikoutelis, P. Paul, Phys. Rev. C **61**, 024613-1 (2000).
9. P. Fröbrich, I.I. Gontchar, N.D. Mavlitov, Nucl. Phys. A **556**, 281 (1993).
10. J. Blocki, Y. Boneh, J.R. Nix, J. Randrup, M. Robel, A.J. Sierk, W.J. Swiatecki, Ann. Phys. (N.Y.) **113**, 330 (1978).
11. S. Pal, T. Mukhopadhyay, Phys. Rev. C **54**, 1333 (1996).
12. Gargi Chaudhuri, S. Pal, Phys. Rev. C **65**, 054612 (2002).
13. H. Hofmann, F.A. Ivanyuk, C. Rummel, S. Yamaji, Phys. Rev. C **64**, 054316 (2001).
14. J. Blocki, F. Brut, T. Srokowski, W.J. Swiatecki, Nucl. Phys. A **545**, 511c (1992).
15. H. Rossner, D.J. Hinde, J.R. Leigh, J.P. Lestone, J.O. Newton, J.X. Wei, S. Elfstrom, Phys. Rev. C **45**, 719 (1992).
16. C.R. Morton, D.J. Hinde, J.R. Leigh, J.P. Lestone, M. Dasgupta, J.C. Mein, J.O. Newton, H. Timmers, Phys. Rev. C **52**, 243 (1995).
17. K.-T. Brinkmann, A.L. Caraley, B.J. Fineman, N. Gan, J. Velkovska, R.L. McGrath, Phys. Rev. C **50**, 309 (1994).
18. M. Brack, J. Damgard, A.S. Jensen, H.C. Pauli, V.M. Strutinsky, C.Y. Wong, Rev. Mod. Phys. **44**, 320 (1972).
19. A.J. Sierk, Phys. Rev. C **33**, 2039 (1986).
20. T. Wada, Y. Abe, N. Carjan, Phys. Rev. Lett. **70**, 3538 (1993).
21. K.T.R. Davies, A.J. Sierk, J.R. Nix, Phys. Rev. C **13**, 2385 (1976).
22. A.J. Sierk, J.R. Nix, Phys. Rev. C **21**, 982 (1980).
23. A.V. Ignatyuk, G.N. Smirenkin, A.S. Tischin, Yad. Fiz. **21**, 485 (1975) (Sov. J. Nucl. Phys. **21**, 255 (1975)).
24. R. Balian, C. Bloch, Ann. Phys. (N.Y.) **60**, 401 (1970).
25. N.D. Mavlitov, P. Fröbrich, I.I. Gonchar, Z. Phys. A **342**, 195 (1992).
26. Gargi Chaudhuri, S. Pal, Phys. Rev. C **63**, 064603 (2001).
27. T. Wada, N. Carjan, Y. Abe, Nucl. Phys. A **538**, 283c (1992).